Species-Specific Stable Isotope Fractionation of Mercury during Hg(II) Methylation by an Anaerobic Bacteria (Desulfobulbus propionicus) under Dark Conditions

ARTICLE *in* ENVIRONMENTAL SCIENCE AND TECHNOLOGY · NOVEMBER 2009

Impact Factor: 5.33 · DOI: 10.1021/es902206j · Source: PubMed

Species-Specific Stable Isotope Fractionation of Mercury during Hg(II) Methylation by an Anaerobic Bacteria (*Desulfobulbus propionicus*) under Dark Conditions

PABLO RODRÍGUEZ-GONZÁLEZ,*,† VLADIMIR N. EPOV,† ROMAIN BRIDOU,‡ EMMANUEL TESSIER,† REMY GUYONEAUD,‡ MATHILDE MONPERRUS,† AND DAVID AMOUROUX*,†

Laboratoire de Chimie Analytique Bio-Inorganique et Environnement, and Equipe Environnement et Microbiologie, Institut Pluridisciplinaire de Recherche sur l'Environnement et les Matériaux (IPREM), Université de Pau et des Pays de l'Adour, UMR CNRS- 5254-IPREM, 2 Avenue Pierre Angot, 64053 Pau, France

Received July 24, 2009. Revised manuscript received November 2, 2009. Accepted November 4, 2009.

This work reports the first results on the stable isotope fractionation of Hg during methylation by anaerobic bacteria under dark conditions. The GC-MC-ICPMS methodology employed is capable of simultaneously measuring the species-specific isotopic composition of different Hg species within the same sample. We have studied Hg isotopic fractionation caused by methylation of Hg(II) standard reference material NIST-3133 in the presence of the pure bacterial strain *Desulfobulbus propionicus* MUD10 (DSM 6523) under fermentative conditions. We have measured the isotopic composition of Hg(II) and monomethyl mercury (MMHg) in these cultures as a function of time and calculated delta-values for both species versus the starting material (NIST-3133) as a delta-zero standard. Two different strategies for the incubation were applied: single sampling cultures and a continuous sampling culture. The results obtained have shown that under the conditions employed in this work the methylation of Hg(II) causes mass-dependent fractionation of the Hg isotopes for both Hg(II) substrate and produced MMHg. Such a process occurred under the exponential growth of the bacteria which preferentially methylate the lighter isotopes of Hg. After 96 h for the continuous culture and 140 h for the single sampling cultures, we observed a change in the fractionation trend in the samples at a similar cell density value (ca. 6.0×10^7 cells mL^{-1}) which suggests the increasing contribution of a simultaneous process balancing methylation extent such as demethylation. Assuming that Rayleigh type fractionation conditions are met before such suppression, we have obtained a $\alpha_{202/198}$ fractionation factor of 1.0026 ± 0.0004 for the single sampling cultures.

* Corresponding author phone +33 (0) 559 407 756; fax: +33 (0) 559 407 781; e-mail: rodriguezpablo@uniovi.es (P.R.-G.); david.amouroux@univ-pau.fr (D.A.).

† Laboratoire de Chimie Analytique Bio-Inorganique et Environnement.

‡ Equipe Environnement et Microbiologie, Institut Pluridisciplinaire de Recherche sur l'Environnement et les Matériaux.

Introduction

The environmental reactivity of Hg is extremely dependent on its chemical form. For example, Hg transfer to the atmosphere occurs via the volatilization of Hg(0), whereas Hg bioaccumulation is due to the greater trophic transfer efficiency of monomethylmercury (MMHg) (*1*). The presence of MMHg in the aquatic environment is due to the biotic or abiotic methylation of Hg(II) caused by specific redox gradients or bacterial activity (*2*). MMHg is able to enter and accumulate in the cytoplasm of phytoplankton cells rather than in the membrane, and its interaction with biomolecules is not limited to S centers but also to C and N centers of DNA bases, pointing out additional mechanisms for the Hg mutagenicity (*3*). MMHg is the most important species involved in the human Hg exposure via fish consumption, and its high toxicity has led to the worldwide control and regulation of the Hg levels in foodstuffs (*4*).

The study of the stable isotope biogeochemistry of Hg has been reported as a powerful tool to track the Hg cycle and pathways in the environment (*5*). However, despite the evidence that Hg mobility and bioaccumulation depends on the chemical form (species) in which Hg is present in the environment, there is a lack of methodologies able to provide a simultaneous determination of the isotopic fractionation of different Hg species within the same environmental sample. Most of the previous studies report total Hg isotopic compositions in the samples (*6*−*8*) whereas only a few of those report the species-specific isotopic fractionation of Hg(0) by its previous isolation using gold amalgamation (*9, 10*) or trapping solutions (*11*). The Hg(II) and MMHg isotopic fractionation during the photoreduction by sunlight (*12*) has been studied using those strategies. Bergquist and Blum (*12*) demonstrated that Hg(II) and MMHg photoreduction causes mass-dependent fractionation (MDF) of Hg isotopes and mass-independent fractionation (MIF) of the odd-mass isotopes. This MIF signal imprinted in the Hg isotope distribution in natural samples can be related to the impact of Hg photoreduction in the environment. In addition, Kritee et al. have shown that both Hg(II) reduction (*13, 14*) and MMHg degradation (*15*) by different Hg(II)-resistant bacterial strains caused exclusively a MDF of the even Hg isotopes.

The study of the different methylation pathways of Hg is critical to acquire a full understanding of the Hg biogeochemical cycle. Previous works have reported the methylation potential of different bacterial strains focusing on sulfate-reducing bacteria (SRB). Those works have confirmed the link between Hg methylation and sulfate reduction (*16, 17*) although the methylation activity can also occur when SRB grow under fermentative conditions (*18*). Hg methylation mechanisms by bacteria are still poorly understood. It has been demonstrated that complete oxidizers methylate mercury via a side reaction of the acetyl-coenzyme A pathway in the cytoplasm (*19*) whereas some incomplete oxidizers can methylate Hg via different pathways independent of the acetyl-coenzyme A (*20*). Also, it has been reported that sulfide concentration influences the Hg bioavailability (*21*), HgS° being the dominant neutral complex controlling the uptake mechanism for inorganic Hg by SRB (*22*). However, Kelly et al. (*23*) showed evidence that Hg(II) uptake by cells is not only driven by passive diffusion of the neutral form $HgCl_2$ but also by an active cell process of different charged and uncharged Hg species. Recently, Schaefer and Morel (*24*) have reported the formation of a mercury−cysteine complex promoting both the uptake of inorganic mercury by the bacteria and the enzymatic formation of methylmercury by

10.1021/es902206j
Published on Web 11/19/2009

SRB. The stable isotope fractionation of Hg(II) during a methylation process has never been studied before and might provide new insights to understand the environmental and biochemical aspects of this important process. The isotopic composition of MMHg in real samples has only been reported in Certified Reference Materials containing 100% MMHg ((*9*), (*12*)) and in environmental samples, such as fish, in which MMHg content is assumed to be 100% (*12*) or by means of tedious offline isolations of MMHg from the matrix by applying numerous sequential extraction steps (*25*). The latter study also did not verify potential Hg isotope fractionation artifacts due to incomplete extraction efficiencies.

This work reports the first results on the isotopic fractionation of Hg during methylation by bacteria in dark conditions. The analytical methodology is based on the coupling of gas chromatography to MC-ICP-MS and on the measurement of isotope ratios from species-specific transient signals (*26*). It provides a lower external precision in the delta values than that obtained using continuous sample introduction techniques such as cold vapor (*5*). However, it is the only available methodology capable of simultaneously measuring the isotopic composition of different Hg species within the same sample. The methodology is applied here for the first time to measure the species-specific isotopic composition of Hg in cultures of the pure bacterial strain *Desulfobulbus propionicus* MUD10 (DSM 6523) which is able to methylate Hg(II) (standard reference material NIST-SRM-3133) when it is incubated under fermentative conditions.

Experimental Section

Microorganism and Culture Conditions. Incubations were performed using the incomplete oxidizer sulfate-reducing bacterial strain *Desulfobulbus propionicus* MUD 10 (DSM 6523). This organism is able to methylate Hg under both sulfate-reducing and fermentative conditions (*20*). Such conditions were selected to prevent the sulfide production during the incubations, as it was demonstrated in a previous work (*21*) and in previous experiments in our laboratory that incomplete recoveries of Hg(II) are obtained when SRB were used for Hg methylation studies, probably due to the complexation of Hg(II). Therefore, to obtain a quantitative recovery of the Hg species in the samples prior to isotope ratio measurements by GC-MC-ICP-MS, we selected fermentative conditions in all the experiments using pyruvate as carbon source and electron acceptor in the presence of the Hg(II) standard reference material NIST-SRM-3133. A nonmethylating biotic control was carried out using the strain *Pseudomonas stutzeri* (ADR04) isolated from the Adour estuary (South West of France) incubated in the presence of NIST-SRM-3133 Hg(II). The incubation conditions and the optimal synthetic medium composition are detailed in the Supporting Information as well as in previous work (*17*).

Mercury Methylation Experiments. All methylation experiments were carried out in the dark using the optimal synthetic medium at 30 °C and pH 7.2. Incubations were performed in acid-precleaned glass material with PTFE stoppers. Two different strategies for incubations (presented in Figure S1) were followed. First, a sampling culture of 100 mL was continuously incubated during 140 h with the Hg(II) standard NIST 3133 at a starting concentration level of 50 ng g^{-1}. In this case, 12 different aliquots were taken at different times from the same incubation vial. The influence of the medium on the Hg(II) methylation was checked by performing an abiotic control incubated under the same conditions (continuous sampling culture) but in the absence of the strain DSM 6523. In addition, the influence of the medium in the presence of living cells and fresh organic matter was studied by replacing the strain DSM 6523 for the nonmethylating strain ADR04 in the continuous sampling culture mode with no electron donors or acceptors to keep a constant pool of living biomass. When continuous sampling cultures were performed, the aliquots were taken with a syringe and they were directly added into a 4 mL volume of 6 N HNO_3 and immediately capped.

The second incubation strategy was based on 24 independent single sampling cultures performed using 10 mL glass vials in which the same medium (spiked with the NIST 3133 standard reference material) was added and incubated. All the sample uptakes and preparation were performed by means of syringes and needles through the PTFE septum to keep anoxic conditions and to avoid any Hg loss. The incubations were stopped by adding 6 N HNO_3 directly to the vial by means of a syringe inserted through the PTFE septum. The inorganic mercury speciation was modeled using the Visual MINTEQ ver. 2.61 software including the chemical composition of the synthetic medium detailed in the Supporting Information at pH 7.2. The major Hg species obtained under these conditions was the neutral $HgCl_2$ (42%) and two anionic species, $HgCl_3^-$(37%) and $HgCl_4^{2-}$ (17%). The total molarity of Cl^- in the media was 0.087 M.

Results and Disscusion

Characterization of the Incubation Conditions, Bacterial Growth, and Hg Speciation. *Characteristics of the Initial Experimental Conditions.* Figure S1 shows a scheme of the preparation of the different incubations performed in this work. A specific control was prepared and analyzed in terms of concentrations and isotopic composition at each stage of the preparation of the different incubation vials. The results regarding the concentration of the Hg(II) NIST 3133 can be seen in Table S2. We can observe that a loss in concentration is produced just after the addition of the strain DSM6523 to the medium. The concentration decreased from the theoretical 100 ppb to approximately 50 ppb and was kept constant until the end of the sample preparation. We can attribute this loss to a possible reduction of Hg(II) and subsequent loss of Hg(0) when adding the strain and/or the associated reductive agents produced during fermentative conditions of the inoculum. Gas partitioning as well as nonquantifiable adsorption of Hg(0) or Hg(II) to the increasing air-exposed wall surface of the initial 0.5 L glass container may also explain this loss. Table S2 shows the isotopic composition of the control samples. Except for Sample C1, we could only perform one measurement because of the limited amount of sample; thus, we cannot conclude that any significant fractionation is occurring in the control samples. A possible isotopic fractionation would nevertheless not alter the purpose of our study, as we are only interested in the isotope variations produced after the initial incubation time. The average of the concentration values of the samples C3 to C6 (46.5 ± 7.6 ng Hg g^{-1}) was taken as an initial reference range of Hg(II) initial concentration in the sample cultures.

Bacterial Growth Condition in Single and Continuous Sampling Cultures. The results obtained in the different cultures can be found in Tables S3 and S4 and in Figures S7 and S8 where we can observe that the samples from the single sampling cultures exhibited an exponential growing phase during the overall experiment with a growth rate value of $\mu = 0.0091$ h^{-1} ($R^2 = 0.97$). The results obtained at the end of the continuous sampling culture indicated that the protein production was higher than that of the last single sampling cultures (61.3 μg mL^{-1} in comparison with 32.0 μg mL^{-1}) and suggest a higher mean growth rate of $\mu = 0.0227$ h^{-1} than in the single sampling cultures. For the biotic control with the strain *Pseudomonas stutzeri* (ADR04), the initial and final value were 4.4 and 12.5 μg mL^{-1}, respectively, indicating that the number of divisions (n) of the bacterial population was equal to unity, whereas for the continuous sampling culture and the single sampling culture this number increased up to 1.7 and 2.8, respectively. The cell densities obtained at the

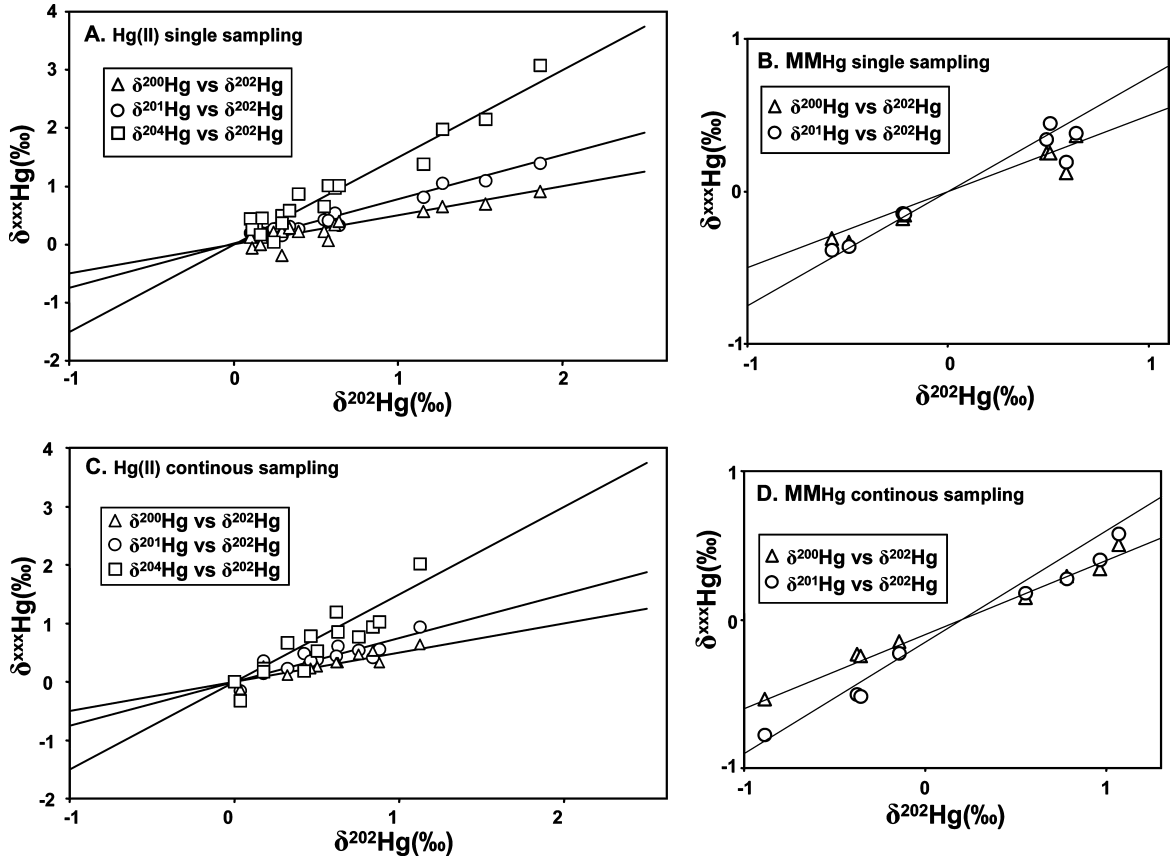

FIGURE 1. Mass dependence of fractionation plotted as δ^{xxx}Hg vs δ^{202}Hg being xxx, 200, 201, and 204 for (A) Hg(II) in the single sampling cultures, (B) MMHg in the single sampling cultures, (C) Hg(II) in the continuous sampling culture, and (D) MMHg in the continuous sampling culture.

end of the incubations were 6.0×10^7 cells mL^{-1} and 1.3×10^8 cells mL^{-1} for the single sampling cultures and for the continuous culture, respectively.

Time Course Evolution of Hg(II) and MMHg Concentrations. The concentrations of the Hg species in the samples were determined by species-specific isotope dilution analysis and are shown in Figure S9 and Tables S3 and S4. The typical precision of this type of speciation analysis is better than 3% RSD (*27*). As can be observed, the concentration of Hg(II) in the single sample cultures fall within the initial concentration interval of 46.5 ± 7.6 ng Hg g^{-1} whereas the MMHg production becomes significant after 54 h (values higher than 1 ng Hg g^{-1}) up to 4.5 ng Hg g^{-1} at the end of the incubation. The continuous sampling culture showed a higher production of MMHg (up to 10 ng Hg g^{-1}) with a more inhomogeneous concentration of Hg(II) through the incubation period, particularly in the last two samples. According to the values of Tables S3 and S4, this higher MMHg concentration also corresponds to a higher production of protein. The Hg species concentration of the biotic and abiotic controls can be seen in Figure S10. Both controls show MMHg values in the range of the blank value (0.51 ± 0.1 ng Hg g^{-1}) throughout all the incubation, but the Hg(II) concentration decreases with time, indicating a continuous and uncontrolled loss. Experiments in our laboratory (*28*) indicated that when the extraction of the Hg species is performed directly in the incubation vial, a 100% recovery of both IHg(II) and MMHg species is obtained. Therefore, a decrease of the Hg(II) concentration is not observed in the individual sampling cultures where the incubation was directly stopped by injecting 6 N HNO_3 through the septum in the same vial to keep the anaerobic conditions and hence possibly avoiding adsorption effects in the glass vial. As observed in Figure S8, the concentration level of the MMHg in the single sampling cultures increases continuously during the incubation, and it is linearly correlated with the protein production value ($R = 0.974$, $p < 10^{-4}$) which is in the optimal physiological activity of the overall bacterial cells in these conditions.

Determination of the Isotopic Fractionation of Hg during Microbial Methylation. *Species-Specific Mass-Dependent Isotopic Fractionation.* The species-specific Hg isotopic compositions obtained for the continuous and single sampling cultures are given in Table S3 and Table S4. Also, Figure 1 shows the three isotope plots obtained for Hg(II) and MMHg in the continuous culture and in the single sampling cultures. All delta values fall within analytical uncertainties on the theoretical mass-dependent fractionation line. These results indicate that the Hg(II) methylation in the single sampling cultures causes MDF of the Hg isotopes 198, 200, 201, and 204 of both Hg(II) and MMHg. Unfortunately, the delta values for 199 cannot be discussed because of lack of validation of this measurement. The precision obtained in the delta values for MMHg was lower because of the extremely low concentration in the samples. Nevertheless, these results indicate that the methylated Hg under the experimental fermentative conditions employed in this work also exhibit a MDF signature. Concerning the fractionation factors, they were calculated employing eq S.4 (Supporting Information) from the δ^{202}Hg delta values of the Hg(II) in both type of incubations.

For the calculation of f (the fraction of reactant Hg(II) remaining), we selected the last sample in which we could exclusively obtain the species-specific isotope ratios of Hg(II) because of a very low amount of MMHg product (see Tables S3 and S4). For the single sampling cultures, the selected reference sample was taken at $t = 51$ h with an initial concentration of Hg(II) of 53.5 ng Hg g^{-1} and a concentration of MMHg product of 1.1 ng g^{-1} (determined by GC-Q-ICPMS).

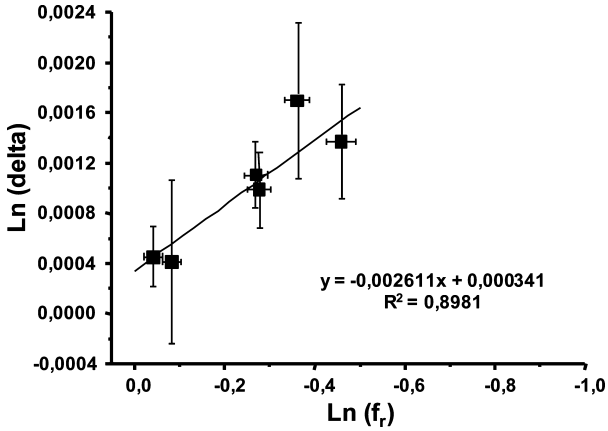

FIGURE 2. Rayleigh plot for the single sampling cultures based on the ^{202}Hg delta values.

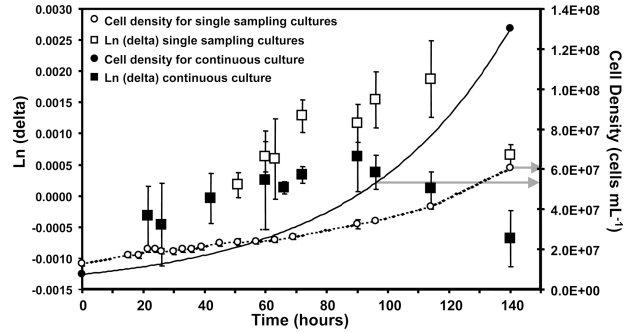

FIGURE 3. $\ln[((1000 + \delta_{Hg(II),t=i}))/((1000 + \delta_{Hg(II),t=0}))]$ as a function of time for the reactant Hg(II) in the single sampling cultures (white squares) and the continuous sampling culture (black squares). Cell densities for the continuous culture (black circles) and the single sample cultures (white circles) are also presented. The cell densities at which the dampening of fractionation is observed is indicated by the gray arrows.

Using the same criteria, the selected initial reference sample for the continuous culture was taken at $t = 36$ h with a 41.7 ng Hg g^{-1} concentration of Hg(II) and a concentration of MMHg of (0.89 ng Hg g^{-1}). Both initial concentrations of Hg(II) were in agreement with the initial reference range of Hg(II) initial concentration in the sample cultures (46.5 ± 7.6 ng Hg g-1). Then the Rayleigh plots for Hg(II) were calculated using the six following samples listed in Table S3 and S4. The last two samples of the continuous culture and the last sample of the single sampling cultures were not considered in these calculations because of a dampening in the fractionation that will be discussed later. In the case of the two last samples of the continuous culture, the lack of recovery of the Hg(II) (see Figure S9B) was an additional argument to reject those samples. This behavior was also observed in the abiotic and biotic controls in which an important decrease in the concentration was observed for both continuous sampling controls.

Figure 2 shows the Rayleigh plot obtained for the single sampling culture using the York method (*29*) which takes into account the individual uncertainty of each data point. The $\alpha_{202/198}$ fractionation factors obtained for the methylation of Hg(II) were $\alpha_{202/198} = 1.0026 \pm 0.0004$ for the single sampling incubations and $\alpha_{202/198} = 1.0016 \pm 0.0020$ for the continuous sampling culture. However, because of a lack of statistical validation of the Rayleigh plot obtained for the continuous sampling culture, the latter fractionation factor was not considered in the discussion. It is worth noting that in some cases the Ln(fr) points in the Rayleigh plots do not occur sequentially in time during the reaction. Some possible reasons may help to explain these results: a lack of sample homogenization in the continuous culture, a different methylation efficiency in the different single sample incubations, or the occurrence of a demethylation process regenerating Hg(II).

Mass-Dependent versus Potential Mass-Independent Isotopic Fractionation. The isotopic composition of both species (Tables S3 and S4) reveal a preferential methylation of the lighter isotopes of Hg(II). The total range of δ^{202}Hg observed in the Hg methylation examined in this study was always below 2‰. Under the conditions employed in this work, we have found that the methylation of Hg(II) by *D. propionicus* (DSM 6523) induce MDF in both reactant (Hg(II)) and product (MMHg) (Figure 1). Recently, it has been discussed (*15*) that significant MIF (especially by the magnetic isotope effect) is unlikely to be observed during any dark microbial Hg transformation pathway. However, Jackson and co-workers (*25*) have reported MIF signatures in natural samples, suggesting that biotic processes can also cause MIF. Our results are in agreement with the works (*13*−*15*) reporting the absence of MIF under dark microbial transformations such as the reduction of Hg(II) to Hg(0) and the degradation of MMHg. This is also proven with the values for Δ^{201}Hg (shown in Tables S2 and S3) which are negligible in comparison with those previously reported (*12*) for photo-induced Hg(II) reduction and photodegradation of MMHg and similar to those obtained for the microbial degradation of MMHg (*15*).

However, the specific limitation of the uncertainty of the GC-MC-ICPMS method does not completely resolve the MIF isotope signature. MIF has been suggested to result from either magnetic interactions (magnetic isotope effect (*30*), MIE) or from nuclear volume effects (*31*) (NV). NV fractionation results in a displacement of the ground electronic energy of an atom or molecule due to the nuclear sizes and shapes of the isotopes whereas MIE is based on the spin conversion principle in intermediate products in a reaction involving Hg radicals. MIE has been proposed as the mechanism involved during the photoreduction of both Hg(II) and MMHg to Hg(0) in the presence of dissolved organic carbon leading to a ^{199}Hg and ^{201}Hg enrichment in the solution relative to MDF (*12*). More recently, Estrade et al. (*32*) re-evaluated nuclear volume scaling factors relative to ^{202}Hg/^{198}Hg for the recommended Hg stable isotope reporting guidelines. The authors reported that the scaling factors obtained by Hahn et al. (*33*) suggested that no ^{204}Hg anomaly is expected during NV fractionation in agreement with previous experimental studies (*12, 34*). If the nuclear volume scaling factor for ^{201}Hg/^{198}Hg reported by Hahn et al. (*33*) (0.6838) is applied in our data reported in Table S4, it can be concluded that our experimental uncertainty on δ^{201}Hg values is too high to resolve MIF because of a NV effect. For example, taking the sample, collected at 15 h, with a δ^{202}Hg of 0.42 ± 0.05 and a δ^{201}Hg of 0.48 ± 0.21 (Table S4) and applying such a scale factor (0.42 × 0.6838), we obtain a theoretically expected δ^{201}Hg value due to nuclear volume isotope effect of 0.28. This example demonstrates that NV fractionation from a MIF signature cannot be discriminated. The ratio of the anomalies Δ^{199}Hg /Δ^{201}Hg has been also employed to discriminate between NV and MIE as a cause of MIF ((*12*), (*32*)). The initial conditions of our experiment (such as the absence of light) do not promote the occurrence of necessary intermediate products during methylation which can lead to the fractionation of isotopes with nuclear spin (such as ^{201}Hg). However, the ratio of the anomalies Δ^{199}Hg /Δ^{201}Hg cannot be employed to confirm this assumption because of lack of validated δ^{199}Hg values in our work.

Time Course Evolution of the Isotopic Fractionation and Potential Processes Involved. Figure 3 shows the $\ln[((1000 + \delta_{,t=i}))/((1000 + \delta_{t=0}))]$ values as a function of time for the reactant Hg(II) in the single sampling cultures and the

continuous sampling culture. The figure also shows the cell density values obtained in each single sampling culture and the exponential curve constructed with the initial and final values of the cell density in the continuous culture. Similarly than the results reported by Kritee et al. ((*13*), (*14*)) for the microbial MMHg degradation and Hg(II) reduction (*15*), we have observed a suppression in the isotopic fractionation at 140 h for the single sampling cultures (33.8 ng Hg(II) g^{-1}, 6.1 $\times$ 10^7 cells mL^{-1}) and at 96 h for the continuous culture (38.5 ng Hg(II) g^{-1}, 5.3 $\times$ 10^7 cells mL^{-1}). Figure 3 shows that the dampening in the fractionation occurs in both experiments at very similar cell densities and that after such dampening, the $\ln[((1000 + \delta_{,t=i}))/((1000 + \delta_{t=0}))]$ values tend to decrease to the initial levels instead of keeping a constant value.

Two observed effects suggest that simultaneous processes different than methylation of Hg(II) are taking place during our experiments. First, some of the ln(fr) points in the Rayleigh plots do not occur sequentially in time during the reaction (see Tables S3 and S4). For the single sampling cultures this effect could be also explained by a different methylation efficiency of the independent incubations, but in the continuous culture the reaction should happen in a forward direction. The second effect is the above-mentioned decrease in the δ^{202}Hg of Hg(II) after the observed dampening in the fractionation. Different processes simultaneous or competitive to methylation may thus be involved during the incubation experiment to explain these results:

(1) Diffusion, uptake, and reaction at the cell interfaces. Koster van Groos et al. (*35*) have recently reported the Hg(0) isotopic fractionation resulting from permeation through a polymeric material, suggesting that diffusion processes through polymer-like materials such as the cell periplasm and membranes can result in large isotope variations. However, this process cannot be identified, as it would alter the measured isotopic signature of the mercury before methylation on either extra- or intracellular fractions. In our study, the bulk culture content was measured including both extra- and intracellular Hg species. Hence, the possible isotope fractionation strictly induced by diffusion or any partition process at the cell interface (uptake, adsorption) cannot alter the measured isotopic composition of Hg(II). When the diffusion is limited due to larger cell density, the important increase of the cell surface area may lead to higher interaction with the Hg species by sorption, complexation, or precipitation by biogenic byproducts (such as proteins) or by the living or dead cell material. However, in the last point of the single sampling cultures the statistically significant decrease in the delta value and the 100% recovery of the Hg species should avoid such nonquantitative effect. If one of these processes would be a limiting step over methylation, it would either suppress the fractionation or preserve the Hg(II) enrichment in the heavier isotopes. Previous works ((*13*), (*14*)) have shown that for the Hg(II) reduction to Hg(0) there is a huge variability in the Hg(II) concentration and the cell density at which the suppression in the fractionation is observed (from 30 to 180 ng Hg(II) g^{-1} and from 10^5 to 10^9 cells mL^{-1}). For Hg(II) methylation, under the conditions employed in this work (35 ng g^{-1}), we have observed the suppression in fractionation at a cell density of approximately 6 $\times$ 10^7 cells mL^{-1} for both types of cultures. These results confirm that the dampening in fractionation is not caused by either an absolute cell density or a particular threshold in Hg(II) concentration and that it depends on the specific selected bacterial strain and on the experimental conditions.

(2) Demethylation of the produced MMHg. Simultaneous methylation of Hg(II) and demethylation of MMHg has been reported in pure culture of *Desulfovibrio desulfuricans* (*36*) as well as many sediment incubation experiments dominated by sulfate reduction specific activity ((*37*), (*38*)). A recent methodological and strain specific survey in our laboratory ((*28*), (*39*)) has demonstrated that similarly to several SRB strains tested in this work, the strain *Desulfobulbus propionicus* DSM6523 is able to simultaneously methylate Hg(II) and demethylate MeHg under sulfate reduction conditions (*39*). In addition, the main pathway involved was an oxidative demethylation which leads to the formation of Hg(II) as the end product. Whereas methylation mostly depends on medium composition (Hg bioavailability) and the cell physiology, demethylation is dependent on methylation (*40*) extent when only Hg(II) has been initially added. Assuming a pseudo-first-order reversible reaction, the demethylation rate should increase with increasing MMHg concentration. Despite the significant uncertainty of the MMHg δ^{202}Hg values, we can observe in Tables S3 and S4 that those values change sign at $t = 90$ h and $t = 72$ h in the single sampling and the continuous cultures, respectively. Such a trend in the MMHg δ^{202}Hg values indicates a dampening in the fractionation occurring before that of Hg(II). In the case of a demethylation process fractionating preferentially lighter isotopes, the δ^{202}Hg values for MMHg would be more affected than those of Hg(II) because of the significant difference in the concentration of both species. Such demethylation would be reflected in a decrease of the δ^{202}Hg values of Hg(II) only after a significant production of MMHg (as observed in Tables S3 and S4).

Extent of the Isotopic Fractionation and Research Implications. The fractionation factor $\alpha_{202/198}$ for the reactant Hg(II) obtained in this work (1.0026 $\pm$ 0.0004) is slightly higher than those obtained for the microbial Hg(II) reduction to Hg(0) (a range of 1.0013−1.0020 was reported as the best estimates of $\alpha_{202/198}$) (*13*). According to these data, both processes involving Hg(II) degradation could leave a different MDF signature in the nondegraded Hg(II). Also the $\alpha_{202/198}$ values obtained in this work are significantly higher than that obtained for the microbial demethylation of MMHg (1.0004 $\pm$ 0.0002) (*15*) and that obtained for the photodegradation of MMHg ($\alpha_{202/198} = 1.0016 \pm 0.0002$) (*12*). According to their distribution coefficients (*41*), the bioavailability of MMHg at high cell densities should be higher than that of Hg(II), and thus higher alpha values for MMHg should be expected for a microbial degradation of MMHg. However, as explained above, it is hard to compare dampening in fractionation and fractionation factors obtained under different experimental conditions, particularly when different bacterial strains are selected and when the differences in the cell densities are so important.

Through a critical evaluation of all the potential bias, this study demonstrates a mass-dependent kinetic fractionation of Hg during methylation under dark anaerobic fermentative conditions. These results open the door to further investigations using other bacterial strains, particularly SRB under different physiological conditions aimed at the development of new stable isotope approaches to study and understand the Hg biogeochemical cycling in the environment in general and, in a more particular basis, the Hg(II) methylation and subsequent MMHg demethylation by bacteria.

Acknowledgments

P.R.G. would like to acknowledge the postdoctoral fellowship from the "Secretaria de Estado de Universidades e Investigacion" of the Spanish Ministry of Education and Science. This work was supported by the ANR (Jeune Chercheur program) and the CNRS/INSU (EC2CO−CYTRIX program) in the framework of the MINAMETA and the RIMES project, respectively. Dr. Jeroen E. Sonke (CNRS Toulouse) is also acknowledged for helpful discussions and comments and for his scientific collaboration. Finally, R.B. and P.R.G. would like to thank Ms. Marie-Lise Biscay from the "Centre

Hospitalier des Pyrénées" (Pau) for her urgent supply of technical material.

Supporting Information Available

Supplementary text, Figures S1−S10 and Tables S1−S4 including stable isotopic data for all experiments are available free of charge via the Internet at http://pubs.acs.org.

Literature Cited

(1) Morel, F. M. M.; Kraepiel, A. M. L.; Amyot, M. The chemical cycle and bioaccumulation of mercury. *Annu. Rev. Ecol. Syst.* **1998**, *29*, 543–566.

(2) Fitzgerald, W. F.; Lamborg, C. H.; Hammerschmidt, C. R. Marine biogeochemical cycling of mercury. *Chem. Rev.* **2007**, *107*, 641–662.

(3) Onyido, I.; Norris, A. R.; Buncel, E. Biomolecule-mercury interactions: Modalities of DNA base-mercury binding mechanisms. Remediation strategies. *Chem. Rev.* **2004**, *104*, 5911–5929.

(4) Dabeka, R.; McKenzie, A. D.; Forsyth, D. S.; Conacher, H. B. S. Survey of total mercury in some edible fish and shellfish species collected in Canada in 2002. *Food Addit. Contam.* **2004**, *21*, 434–440.

(5) Blum, J. D.; Bergquist, B. A. Reporting of variations in the natural isotopic composition of mercury. *Anal. Bioanal. Chem.* **2007**, *388*, 353–359.

(6) Lauretta, D. S.; Klaue, B.; Blum, J. D.; Buseck, P. R. Mercury abundances and isotopic compositions in the Murchinson (CM) and Allende (CV) carbonaceous chondrites. *Geochim. Cosmochim. Acta* **2001**, *65*, 2807–2818.

(7) Hintelmann, H.; Lu, S. High precision isotope ratio measurements of mercury isotopes in cinnabar ores using multi-collector inductively coupled plasma mass spectrometry. *Analyst* **2003**, *128*, 635–639.

(8) Ridley, W. I.; Stetson, S. J. A review of the isotopic composition as an indicator of the natural and anthropogenic behavior of mercury. *Appl. Geochem.* **2006**, *21*, 1889–1899.

(9) Xie, Q. L.; Lu, S. Y.; Evans, D.; Dillon, P.; Hintelmann, H. High precision Hg isotope analysis of environmental samples using gold trap-MC-ICP-MS. *J. Anal. At. Spectrom.* **2005**, *20*, 515–522.

(10) Sonke, J. E.; Zambardi, T.; Toutain, J. P. Indirect gold trap-MC-ICP-MS coupling for Hg stable isotope analysis using a syringe injection interface. *J. Anal. At. Spectrom.* **2008**, *23*, 569–573.

(11) Zheng, W.; Foucher, D.; Hintelmann, H. Mercury isotope fractionation during volatilization of Hg(0) from solution into the gas phase. *J. Anal. At. Spectrom.* **2007**, *22*, 1097–1104.

(12) Bergquist, B. A.; Blum, J. D. Mass-dependent and -independent fractionation of Hg isotopes by photoreduction in aquatic systems. *Science* **2007**, *318*, 417–420.

(13) Kritee, K.; Blum, J. D.; Johnson, Bergquist B.A.; , M. W.; Barkay, T. Mercury stable isotope fractionation during reduction of Hg(II) to Hg(0) by mercury resistant microorganisms. *Environ. Sci. Technol.* **2007**, *41*, 1889–1895.

(14) Kritee, K.; Blum, J. D.; Barkay, T. Mercury stable isotope fractionation during reduction of Hg(II) by different microbial pathways. *Environ. Sci. Technol.* **2008**, *42*, 9171–9177.

(15) Kritee, K.; Barkay, T.; Blum, J. D. Mass dependent stable isotope fractionation of mercury during *mer* mediated microbial degradation of monomethylmercury. *Geochim. Cosmochim. Acta* **2009**, *73*, 1285–1296.

(16) Compeau, G. C.; Bartha, R. Sulfate-reducing bacteria: principal methylators of mercury in anoxic estuarine sediment. *Appl. Environ. Microbiol.* **1985**, *50*, 498–502.

(17) Ranchou-Peyruse, M.; Monperrus, M.; Bridou, R.; Duran, R.; Amouroux, D.; Salvado, J. C.; Guyoneaud, R. Overview of mercury methylation capacities among anaerobic bacteria including representatives of the sulphate-reducers: implications for environmental studies. *Geomicrobiol. J.* **2009**, *26*, 1–8.

(18) King, J. K.; Kostka, J. E.; Frischer, M. E.; Saunders, F. M. Sulfate-reducing bacteria methylate mercury at variable rates in pure culture and in marine sediments. *Appl. Environ. Microbiol.* **2000**, *66*, 2430–2437.

(19) Choi, S. C.; Bartha, R. Cobalamin-mediated mercury methylation by *Desulfovibrio desulfuricans* LS. *Appl. Environ. Microbiol.* **1993**, *59*, 290–295.

(20) Ekstrom, E. B.; Morel, F. M. M.; Benoit, J. M. Mercury methylation independent of the acetyl-coenzyme A pathway in sulfate reducing bacteria. *Appl. Environ. Microbiol.* **2003**, *69*, 5414–5422.

(21) Benoit, J. M.; Gilmour, C. C.; Mason, R. P. Aspects of bioavailability of mercury for methylation in pure cultures of *Desulfobulbus propionicus* (1pr3). *Appl. Environ. Microbiol.* **2001**, *67*, 51–58.

(22) Benoit, J. M.; Gilmour, C. C.; Mason, R. P.; Heyes, A. Sulfide controls on mercury speciation and bioavailability to methylating bacteria in sediment pore waters. *Environ. Sci. Technol.* **2001**, *33*, 951–957.

(23) Kelly, C. A.; Rudd, J. W. M.; Holoka, M. H. Effect of pH on mercury uptake by an aquatic bacterium: implications for Hg cycling. *Environ. Sci. Technol.* **2003**, *37*, 2941–2946.

(24) Schaefer, J. K.; Morel, F. M. M. High methylation rates of mercury bound to cysteine by *Geobacter sulfurreducens*. *Nat. Geosci.* **2009**, *2*, 123–126.

(25) Jackson, T. A.; Whittle, D. M.; Evans, M. S.; Muir, D. C. G. Evidence for mass-independent and mass-dependent fractionation of the stable isotopes of mercury by natural processes in aquatic ecosystems. *Appl. Geochem.* **2008**, *23*, 547–571.

(26) Epov, V. N.; Rodríguez-Gonzalez, P.; Sonke, J. E.; Tessier, E.; Amouroux, D.; Maurice Bourgoin, L.; Donard, O. F. X. Simultaneous determination of species-specific isotopic fractionation of Hg by Gas Chromatography coupled to Multicollector ICP-MS. *Anal. Chem.* **2008**, *80*, 3530–3538.

(27) Rodríguez-González, P.; Monperrus, M.; Garcia Alonso, J. I.; Amouroux, D.; Donard, O. F. X. Comparison of different numerical approaches for multiple spiking species-specific isotope dilution analysis exemplified by the determination of butyltin species in sediments. *J. Anal. At. Spectrom.* **2007**, *22*, 1373–1382.

(28) Bridou, R.; Monperrus, M.; Rodriguez-Gonzalez, P.; Ranchou-Peyruse, M.; Bouchet., S.; Tessier, E.; Caumette, P.; Amouroux, D.; Guyoneaud, R. Mercury methylation capacities among anaerobic bacteria including experimental and analytical aspects. Presented at the 9th International Conference on Mercury as a Global Pollutant, Guizhou, China, June 2009.

(29) York, D. Least-squares fitting of a straight line. *Can. J. Phys.* **1966**, *44*, 1076–1086.

(30) Buchachenko, A. L.; Kouznetsov, D. A.; Shishkov, A. V. Spin biochemistry: magnetic isotope effect in the reaction of creatine kinase with CH_3HgCl. *J. Phys. Chem. A* **2004**, *108*, 707–710.

(31) Schauble, E. A. Role of nuclear volume in driving equilibrium stable isotope fractionation of mercury, thallium and other very heavy elements. *Geochim. Cosmochim. Acta* **2007**, *71*, 2170–2189.

(32) Estrade, N.; Carignan, J.; Sonke, J. E.; Donard, O. F. X. Mercury isotope fractionation during liquid-vapor evaporation experiments. *Geochim. Cosmochim. Acta* **2009**, *73*, 2693–2711.

(33) Hahn, A. A.; Miller, J. P.; Powers, R. J.; Zehnder, A.; Rushton, A. M.; Welsh, R. E.; Kunselman, A. R.; Roberson, P.; Walter, H. K. Experimental study of muonic X-Ray transitions in mercury isotopes. *Nucl. Phys.* **1979**, *A314*, 361–386.

(34) Ghosh, S.; Xu, Y. F.; Humayun, M.; Odom, L. Mass-independent fractionation of mercury isotopes in the environment. *Geochem. Geophys. Geosyst.* **2008**, *9*, . doi:, 10.1029/2007GC001827.

(35) Koster van Groos, P. G.; Esser, B. K.; Williams, R.; Hunt, J. R. Mercury isotope fractionation due to permeation of a PVC polymer. *Geochim. Cosmochim. Acta* **2009**, *73*, A687.

(36) Pak, K. R.; Bartha, R. Mercury methylation and demethylation in anoxic lake sediments and by strictly anaerobic bacteria. *Appl. Environ. Microbiol.* **1998**, *64*, 1013–1017.

(37) Oremland, R. S.; Culbertson, C. W.; Winfrey, M. R. Methylmercury decomposition in sediments and bacterial cultures: involvement of methanogens and sulfate reducers in oxidative demethylation. *Appl. Environ. Microbiol.* **1991**, *57*, 130–137.

(38) Martín-Doimeadios, R. C. R.; Tessier, E.; Amouroux, D.; Guyoneaud, R.; Duran, R.; Caumette, P.; Donard, O. F. X. Mercury methylation/demethylation and volatilization pathways in estuarine sediment slurries using species-specific enriched stable isotopes. *Mar. Chem.* **2004**, *90*, 107–123.

(39) Perrot, V; Bridou, R.; Tessier, E.; Rodriguez-Gonzalez, P.; Epov, V. N.; Monperrus, M.; Guyoneaud, R.; Amouroux, D. Investigation of mercury methylation routes combining species-specific isotopic tracers and isotopic fractionation measurements. *Geochim. Cosmochim. Acta* **2009**, *73*, A1015.

(40) Barkay, T.; Miller, S. M.; Summers, A. O. Bacterial mercury resistance from atoms to ecosystems. *FEMS Microbiol. Rev.* **2003**, *27*, 355–384.

(41) Hammerschmidt, C. R.; Fitzgerald, W. F. Methylmercury cycling in sediments on the continental shelf of southern New England. *Geochim. Cosmochim. Acta* **2006**, *70*, 918–930.

ES902206J